nature portfolio

https://doi.org/10.1038/s41550-022-01702-2

Supplementary information

Stochastic accretion of the Earth

In the format provided by the
authors and unedited

Supplementary Information.

Stochastic accretion of the Earth

Paolo A. Sossi[1], Ingo L. Stotz[2], Seth A. Jacobson[3], Alessandro Morbidelli[4], Hugh St.C. O'Neill[5]

[1] Institute of Geochemistry and Petrology, ETH Zürich, CH-8092, Zürich, Switzerland
[2] Institut für Geophysik, Ludwig-Maximilians-Universität München, Münich, Germany
[3] Department of Earth and Environmental Sciences, Michigan State University, East Lansing, MI 48824, USA
[4] Laboratoire Lagrange, UMR7293, Université de Nice Sophia-Antipolis, CNRS, Observatoire de la Côte d'Azur, Boulevard de l'Observatoire, 06304 Nice Cedex 4, France
[5] School of Earth, Atmosphere and Environment, Monash University, Melbourne, VIC 3800, Australia

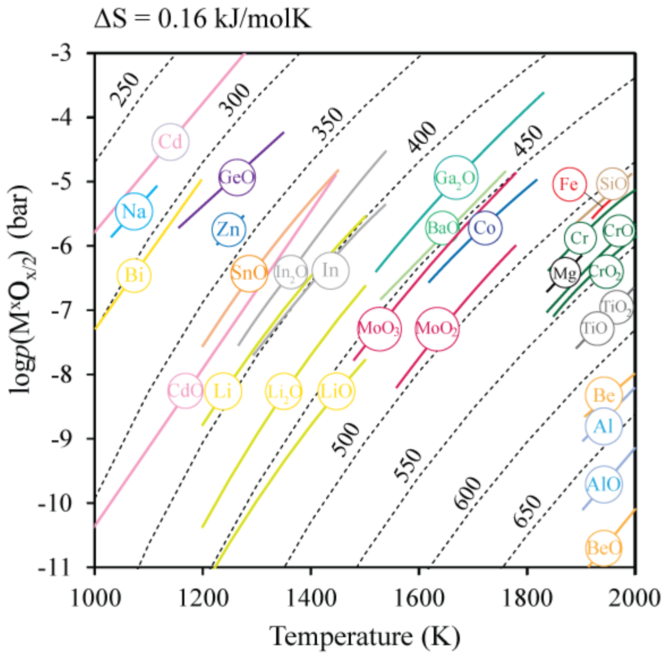

Supplementary Figure 1 | Equilibrium partial pressures of real elements and their fictive counterparts used in the simulations. The logarithm of equilibrium partial pressures (in bar) of metal- and metal-oxide species above pure metal oxides (after ref. 66) determined by thermodynamic measurements. Overlain on these data is the model used herein to calculate vapour pressures of fictive elements, in which the ΔS of vaporisation is constant (0.16 kJ/molK) while the ΔH changes according to element volatility. Curves calculated using eq. 15 are shown as dashed black lines, with the corresponding value of ΔH (*Supplementary Table 1*).

Supplementary Table 1 | Abundances of fictive elements and thermodynamic quantities for

their vaporisation. The thermodynamic properties (ΔH, enthalpy; and ΔS, entropy) of the generalised vaporisation reaction (eq. 11) are shown for the 30 fictive elements defined according to their 50 % nebular condensation temperature (T_c^{50}). Also shown are their initial mole fractions, *x*, in a body that has its full complement of each element. Mole fractions are predicted according to a Gaussian curve centred at 1350 K, in order to produce total pressures that match those for the bulk silicate Earth (BSE, ref. 6; *Supplementary Figure 2*). The activity coefficient, γ, is set to unity for all elements, thus *x* = *a* (activity).

Element T_c^{50} (K)	ΔH (kJ)	ΔS (kJ/molK)	$x_{i,\text{ initial}}$	*n*
1800	736.0	0.16	9.85E-06	2
1750	715.5	0.16	8.25E-05	2
1700	695.1	0.16	5.38E-04	2
1650	674.7	0.16	2.72E-03	2
1600	654.2	0.16	1.07E-02	2
1550	633.8	0.16	3.24E-02	2
1500	613.3	0.16	7.67E-02	2
1450	592.9	0.16	1.38E-01	2
1400	572.4	0.16	1.92E-01	2
1350	552.0	0.16	2.05E-01	2
1300	531.5	0.16	1.68E-01	2
1250	511.1	0.16	1.03E-01	2
1200	490.7	0.16	4.76E-02	2
1150	470.2	0.16	1.74E-02	2
1100	449.8	0.16	4.83E-03	2
1050	429.3	0.16	9.77E-04	2
1000	408.9	0.16	1.49E-04	2
950	388.4	0.16	1.85E-05	2
900	368.0	0.16	1.64E-06	2
850	347.6	0.16	1.08E-07	2
800	327.1	0.16	5.69E-09	2
750	306.7	0.16	2.27E-10	2
700	286.2	0.16	7.07E-12	2
650	265.8	0.16	1.72E-13	2
600	245.3	0.16	2.99E-15	2
550	224.9	0.16	3.52E-17	2
500	204.4	0.16	3.70E-17	2
450	184.0	0.16	2.48E-21	2
400	163.6	0.16	1.94E-23	2
350	143.4	0.16	1.48E-25	2

Supplementary Table 2 | CI-, Mg-normalised abundances of the elements in the bulk silicate Earth (BSE) and Vesta and their nebular condensation temperatures. Only nominally lithophile elements (*N* = 36) were considered herein because core formation, which is not accounted for in the model, is expected to cause depletion additional to that resulting from volatile loss. Condensation temperatures are taken from refs. 22, 76 and 23, while elemental abundances for the BSE (and their uncertainties) are from ref. 6. Element concentrations for Vesta are determined from their measured abundances in four pristine, non-cumulate Eucrites (Pasamonte, Bouvante, Juvinas and Bereba)[75] by normalisation of a volatile element to a refractory element with similar incompatibility during mantle melting, or, from an average (Zn and Mn). On the basis that Mn is non-depleted normalised Mg- and to CI chondrites, all elements with higher T_c^{50} are also presumed to be present in chondritic proportions.

Element	T_c^{50} (K)[22,76]	T_c^{50} (K)[23]	CI-, Mg-normalised (BSE)[6]	1*s*	Method	CI-, Mg-normalised (Vesta)[75]	1*s*
Zr	1741	1722	1.230	0.012	Assumed	1.000	0.100
Hf	1684	1720	1.229	0.090	Assumed	1.000	0.100
Th	1659	1630	1.183	0.106	Assumed	1.000	0.100
Sc	1659	1541	1.201	0.083	Assumed	1.000	0.100
Ho	1659	1630	1.206	0.121	Assumed	1.000	0.100
Gd	1659	1630	1.234	0.027	Assumed	1.000	0.100
Al	1653	1652	1.210	0.084	Assumed	1.000	0.100
U	1610	1609	1.222	0.110	Assumed	1.000	0.100
Nd	1602	1630	1.230	0.085	Assumed	1.000	0.100
La	1578	1615	1.220	0.086	Assumed	1.000	0.100
Ta	1573	1546	1.281	0.043	Assumed	1.000	0.100
Ca	1517	1535	1.223	0.062	Assumed	1.000	0.100
Yb	1487	1528	1.221	0.090	Assumed	1.000	0.100
Ba	1455	1423	1.228	0.138	Assumed	1.000	0.100
Be	1452	1551	1.276	0.062	Assumed	1.000	0.100
Mg	1336	1343	1	0	-	1.000	-
Si	1265[76]	1314	0.857	0.002	Assumed	1.000	0.100
Mn	1158	1123	0.235	0.021	Avg. Eucrites	1.019	0.046
Li	1142	1148	0.470	0.043	Li/Yb	0.778	0.118
K	915[76]	993	0.207	0.025	K/U	0.073	0.010
Ga	968	1010	0.196	0.004	Ga/Al	0.028	0.003
Na	960[76]	1035	0.224	0.005	Na/Yb	0.082	0.021
Cl	400[76]	472	0.019	0.005	-	-	-
B	908	740	0.145	0.046	-	-	-
Rb	800	752	0.113	0.006	Rb/La	0.009	0.001
Cs	799	593	0.041	0.020	Rb/Cs = 30±5	0.005	0.001
Bi	746	480	0.012	0.005	-	-	-
F	734	674	0.186	0.050	-	-	-
Pb	727	495	0.030	0.002	-	-	-
Zn	650[76]	704	0.072	0.002	Avg. Eucrites	0.002	0.001
Sn	704	604	0.037	0.006	-	-	-
Cd	652	502	0.041	0.006	Cd/Zn = 0.0019±0.001	0.002	0.002
Br	546	420	0.010	0.004	-	-	-
In	535	492	0.100	0.015	In/Y	0.003	0.001
I	535	390	0.006	0.002	-	-	-
Tl	532	365	0.013	0.002	Tl/La	1.6e-4	7e-5

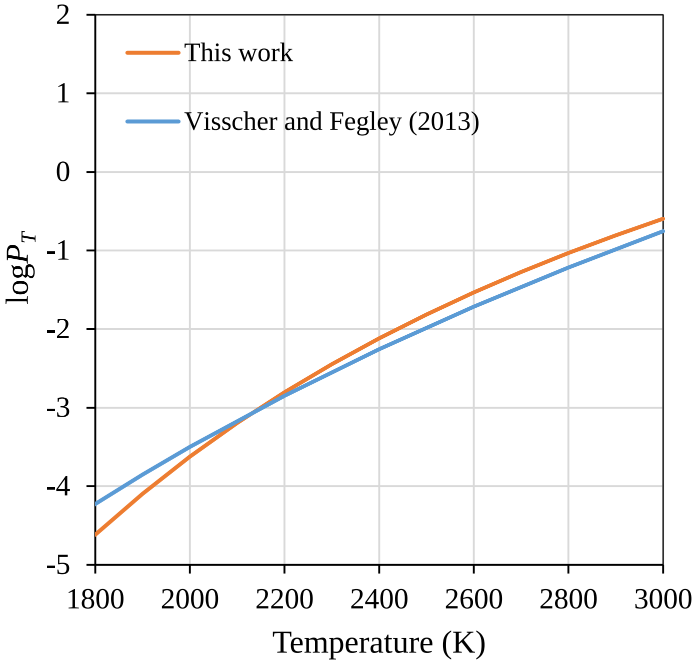

Supplementary Figure 2 | The evolution of total pressure with temperature above a magma ocean. The pressures are calculated for this work using the parameters listed in *Supplementary Table 1* (orange line) via the summation of the partial pressures of the individual elements. Total pressure for the model of ref. 66, blue line) are those above the bulk silicate Earth.

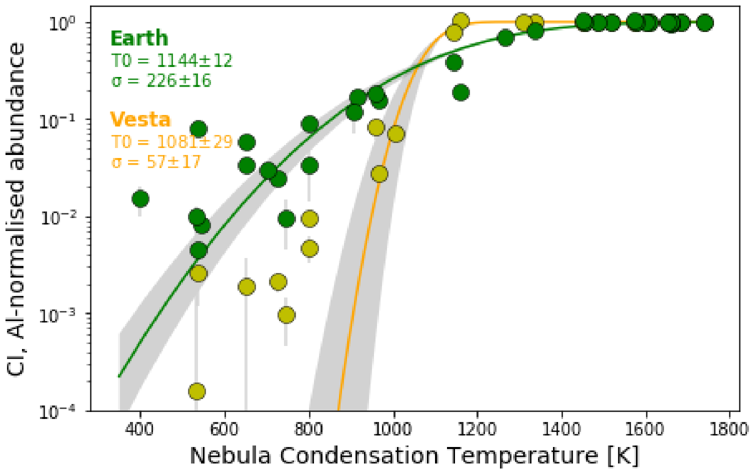

Supplementary Figure 3 | The abundances of lithophile elements in the mantles of the Earth and Vesta shown on a logarithmic scale. This is an alternative representation of Fig. 1. It illustrates that the cumulative normal distribution fit to the abundances of the BSE holds at low T_c^{50}. Elements with T_c^{50} < 800 K in Vesta are predicted to be in lower abundances than those determined from non-cumulate eucrites (*Supplementary Table 2*). This mismatch is partly owing to the lower weighting given to these elements in the fitting algorithm, due to their large uncertainties (*Supplementary Table 2*). However, it cannot be excluded that these elements do reflect their Vestan mantle abundances. In this case, the misfit may be attributed to addition of volatile-rich components to Vesta, akin to a 'late veneer'. Alternative possibilities include terrestrial contamination of these elements during laboratory analysis. Because small bodies such as Vesta have accumulated relatively little mass, they are more likely to deviate from a perfect cumulative normal distribution arising from collection of material with variable compositions. Nevertheless, this figure shows that volatile elements are essentially absent in Vesta relative to CI chondrites, and its composition is well approximated by a step-function.

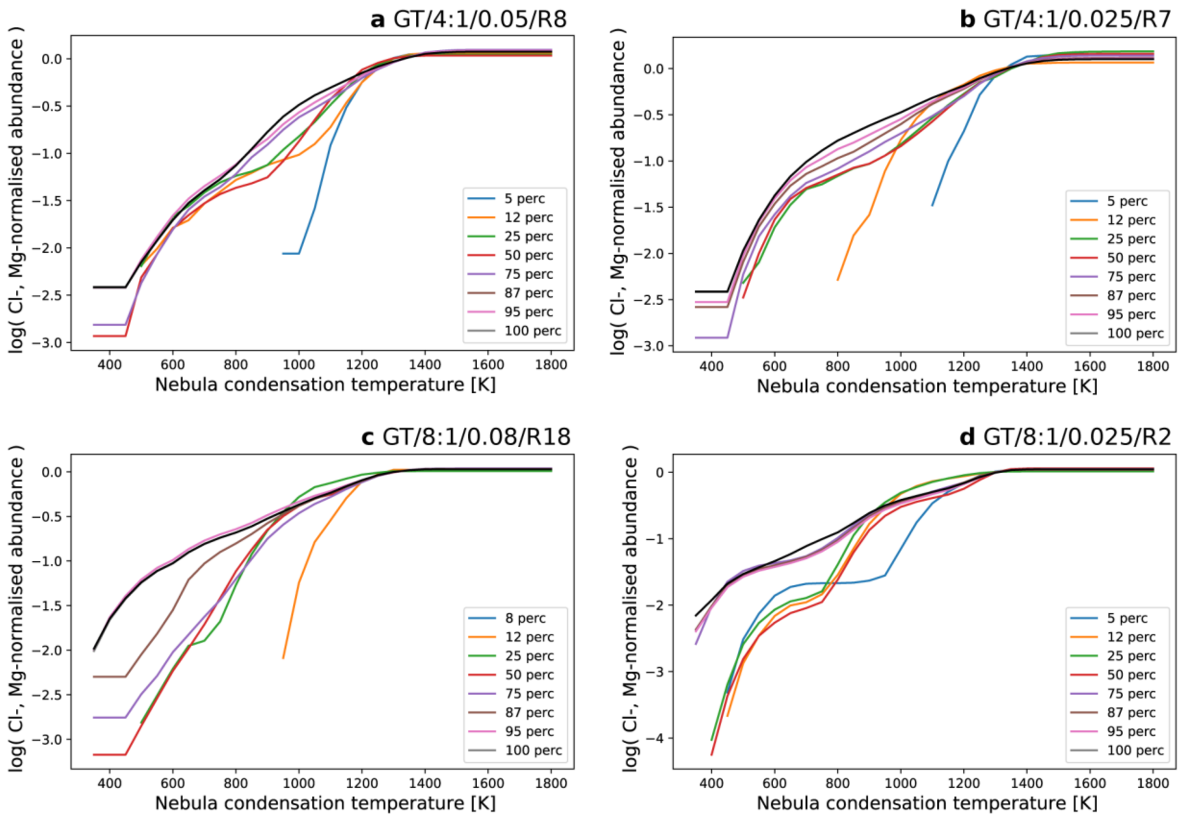

Supplementary Figure 4 | Evolution of the bulk composition of the Earth as a function of mass accreted for four N-body simulations. CI-, Mg-normalised elemental abundances in the BSE modelled as a function of 50% nebular condensation temperatures for a set of simulations with constant $\dot{M}$, σ_{embryo} and m_i, equal to 1×10^{-7} solar masses/yr, 87 K and 33.5 g/mol, respectively. The curves correspond to the bulk composition of the growing Earth at different stages of its growth, expressed as a function of its total mass (in %). Notable is the evolution from steep, step-function-like patterns at early stages of growth (<25 %) to smoother patterns with higher relative abundances of volatile elements (low T_c^{50}) during the latter stages.

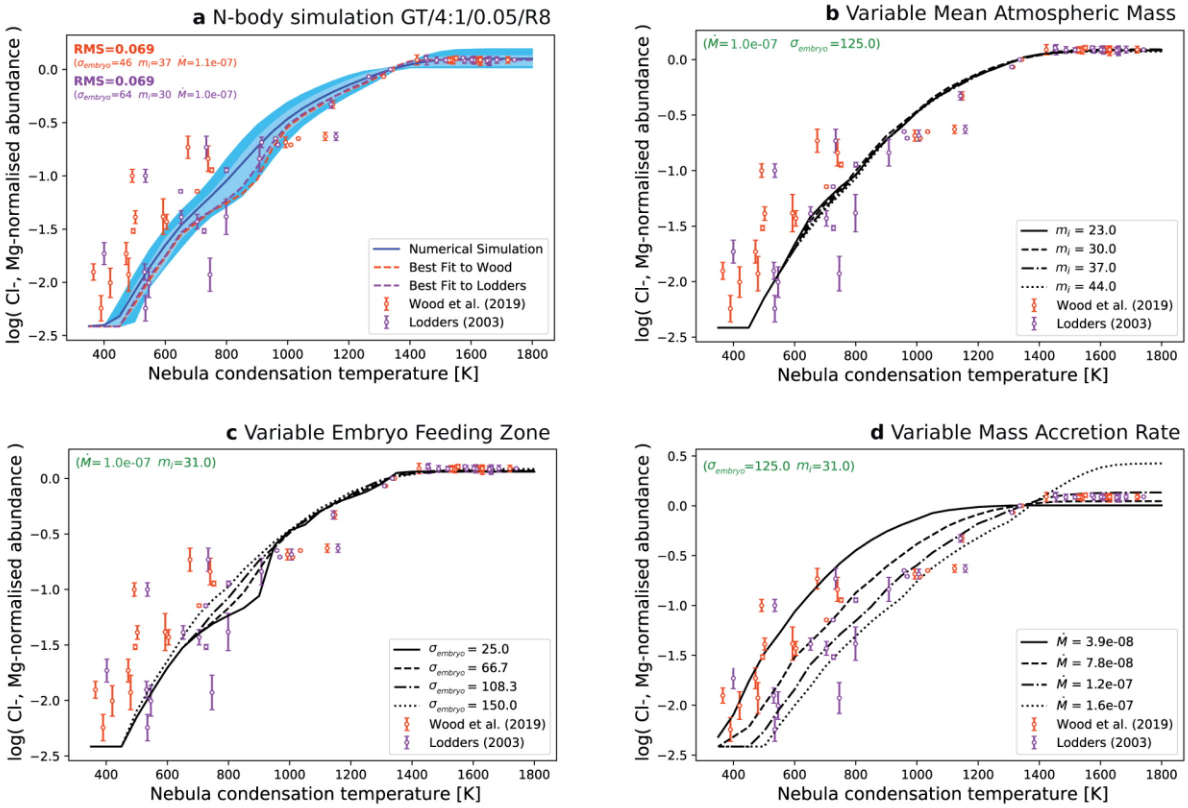

Supplementary Figure 5 | The influence of each of the three random variables on the resultant element depletion pattern of the fully-accreted Earth. a Modelled abundances of 1000 Monte Carlo simulations showing the mean value (solid black line), best-fit value (black dashed line), 75th to 25th percentile (blue field) and 90th to 10th percentile (dark blue field) together with the abundances in the bulk silicate Earth (BSE) as a function of condensation temperature (red[23]; purple[22,76]). In parts **b**, **c**, and **d**, two variables are held constant while the remaining one, that is; **b** atmospheric mass (m_i), **c** embryo feeding zone (σ_{embryo}), and **d** mass accretion rate ($\dot{M}$) is varied to quantify its effect on elemental abundances. Atmospheric molar mass has only a marginal effect on elemental abundances, indicating that atmospheric loss is ineffective in controlling elemental budgets on Earth. Increasing the temperature distribution of embryo feeding zones has the effect of 'smoothing out' irregularities in the pattern as a function of T_c[50]. Mass accretion rate controls the elemental budgets of the initial planetesimals and embryos. As all abundances must sum to 1, depletion in volatile elements for higher mass accretion rates is compensated for by an enrichment in the remaining refractory elements relative to the initial (CI) composition. This is manifest as log(CI-, Mg-normalised depletion factors > 1 (compare dashed and solid lines). For reference, values of CI-, Mg-normalised refractory lithophile elements are ~1.21 in the bulk silicate Earth[6].